



Contents lists available at SciVerse ScienceDirect

Radiation Measurements

journal homepage: www.elsevier.com/locate/radmeas

Modeling of the shape of infrared stimulated luminescence signals in feldspars

Vasilis Pagonis^{a,*}, Mayank Jain^b, Andrew S. Murray^c, Christina Ankjærgaard^d, Reuven Chen^e^a McDaniel College, Physics Department, Westminster, MD 21157, USA^b Radiation Research Division, Risø National Laboratory for Sustainable Energy, Technical University of Denmark, DK-4000 Roskilde, Denmark^c Nordic Laboratory for Luminescence Dating, Department of Earth Science, Aarhus University, Risø National Laboratory for Sustainable Energy, DK-4000 Roskilde, Denmark^d Netherlands Centre for Luminescence Dating, Technical University of Delft, The Netherlands^e Raymond and Beverly Sackler School of Physics and Astronomy, Tel Aviv University, Tel Aviv 69978, Israel

ARTICLE INFO

Article history:

Received 20 September 2011

Received in revised form

30 January 2012

Accepted 24 February 2012

Keywords:

Infrared stimulated luminescence

IRSL

Feldspars

Power law of luminescence

Kinetic rate equations

Kinetic model

Tunneling

ABSTRACT

This paper presents a new empirical model describing infrared (IR) stimulation phenomena in feldspars. In the model electrons from the ground state of an electron trap are raised by infrared optical stimulation to the excited state, and subsequently recombine with a nearest-neighbor hole via a tunneling process, leading to the emission of light. The model explains the experimentally observed existence of two distinct time intervals in the luminescence intensity; a rapid initial decay of the signal followed by a much slower gradual decay of the signal with time.

The initial fast decay region corresponds to a fast rate of recombination processes taking place along the infrared stimulated luminescence (IRSL) curves. The subsequent decay of the simulated IRSL signal is characterized by a much slower recombination rate, which can be described by a power-law type of equation.

Several simulations of IRSL experiments are carried out by varying the parameters in the model. It is found that the shape of the IRSL signal is remarkably stable when the kinetic parameters are changed within the model; this is in agreement with several previous studies of these signals on feldspars, which showed that the shape of the IRSL curves does not change significantly under different experimental conditions. The relationship between the simulated IRSL signal and the well-known power-law dependence of relaxation processes in solids is also explored, by fitting the IRSL signal at long times with a power-law type of equation. The exponent in this power-law is found to depend very weakly on the various parameters in the model, in agreement with the results of experimental studies. The results from the model are compared with experimental IRSL curves obtained using different IR stimulating power, and good quantitative agreement is found between the simulation results and experimental data.

© 2012 Elsevier Ltd. All rights reserved.

1. Introduction

The phenomenon of “anomalous fading” in feldspar samples has been studied extensively both experimentally and by modeling, due to its importance in dating studies of these materials (Wintle, 1973; Visocekas, 1985; Templer, 1986; Duller and Bøtter-Jensen, 1993; Bøtter-Jensen et al., 2003). These studies have suggested that anomalous fading is due to quantum mechanical tunneling from the ground state of the trap (Huntley and Lamothe, 2001; Poolton et al., 2002a, b; Li and Li, 2008; Kars et al., 2008; Larsen et al., 2009; Li and Li, 2010 and references therein). Furthermore, it has been shown that this ground state tunneling process in

various materials can be described by power-law decay (Delbecq et al., 1974; Huntley, 2006). Some studies have suggested that in K-feldspars the infrared stimulated luminescence (IRSL) signal originates from a single trap corresponding to the thermoluminescence peak at ~ 400 °C (as measured with a heating rate of 5 °C/s) (Baril, 2002; Baril and Huntley, 2003; Murray et al., 2009).

The experimental and modeling work by Poolton et al. (2002a, b, 2009) and more recently by Ankjærgaard et al. (2009) and Jain and Ankjærgaard (2011), provide solid understanding of the transport processes giving rise to the IRSL from feldspars. These complex processes are believed to consist of localized recombination by tunneling from the excited state of the trap, as well as charge migration through the conduction band-tail states into the recombination centre. The available experimental data is consistent with band-tails occupying a continuum of energy states from ~ 0.4 eV below the conduction band (Poolton et al., 2009). The

* Corresponding author. Tel.: +1 410 857 2481; fax: +1 410 386 4624.
E-mail address: vpagonis@mcDaniel.edu (V. Pagonis).

continuous-wave IRSL signals (CW–IRSL, also known as “infrared shine down” curves) from feldspars, are known to have a remarkably stable shape. Their shape changes very little with experimental conditions like the irradiation dose and preheat temperature. However, significant changes take place in the CW–IRSL signal shape when the intensity of stimulating IR light is varied experimentally (Thomsen et al., 2008, 2011). It is also noted that significant but smaller changes take place in the CW–IRSL when the stimulation temperature is varied (see e.g. and Jain and Ankjærgaard, 2011; and references therein).

CW–IRSL signals from feldspars are known to decay in a non-exponential manner. Bailiff and Poolton (1991) showed that the IRSL decay follows a power-law. Poolton et al. (1994) explained IRSL in feldspars using a donor–acceptor model, in which electron tunneling occurs from the excited state of the IRSL trap at about 1.4 eV Poolton et al. (1995, 2002a, b) refined this model by including the possibility of charge transfer from the excited state of the IRSL trap into the band-tail states. Thomsen et al. (2008) pointed out that this model implies that the IRSL decay curve is a function of tunneling probability, which is exponentially related to the distance between the donor–acceptor recombination pair. These authors also suggested that in this model, the beginning of the IRSL decay curve originates with the luminescence emitted from close donor–acceptor pairs, while the end of the IRSL curve most likely represents the tunneling of distant pairs.

In this paper we present a new kinetic model based on localized electronic transitions, in an attempt to describe the phenomenon of tunneling in feldspars. This model is based on a new empirical function used to describe variation in the tunneling probability with time in feldspars. Our goal is to compare the results from the model with experimental CW–IRSL data, and to attempt a characterization of the different parts of the IRSL decay curves from feldspars. Furthermore, the model provides us with an insight from the various processes taking place during the measurement of IRSL signals in feldspars at room temperature.

2. The new tunneling model for feldspars

The purpose of this paper is to simulate IRSL signals from feldspars, also known as “infrared shine down” curves.

In the model shown in Fig. 1 we simulate IRSL experiments, by assuming that IR stimulation does not raise any electrons into the conduction band (CB), and by neglecting the effect of the band-tail states. Instead, all transitions take place within the locality of the electron–hole (e–h) pair. The IR stimulation raises electrons from the ground state into the excited state (transition 1); some of these

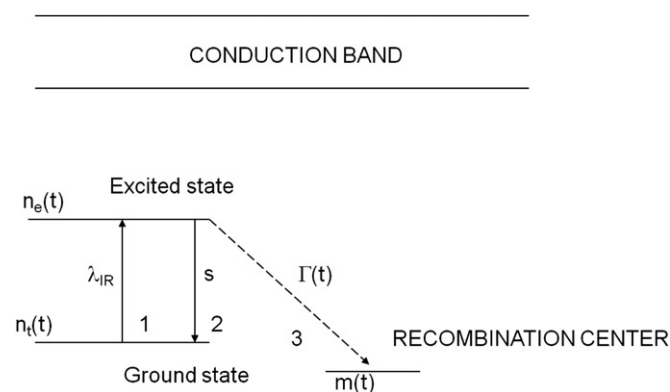


Fig. 1. The electronic transitions taking place during the infrared stimulation of feldspar samples. Electrons are excited by the IR stimulation from the ground state into the excited state of the electron trap, and tunneling takes place from the excited state into the recombination center.

electrons will be retrapped in the ground state (transition 2), while others will recombine radiatively with holes (transition 3).

The various transitions in the model are shown in Fig. 1, and the equations in the model are:

$$\frac{dn_t}{dt} = -\lambda_{IR}n_t(t) + n_e(t)s \quad (1)$$

$$\frac{dn_e}{dt} = \lambda_{IR}n_t(t) - n_e(t)s - n_e(t)\Gamma \quad (2)$$

$$L(t) = -dm/dt = n_e(t)\Gamma \quad (3)$$

In these equations $n_t(t)$ and $n_e(t)$ represent the concentrations of electrons at any instant in the ground state and the excited state, correspondingly. The term $\lambda_{IR}n_t(t)$ represents the rate of change of $n_t(t)$ due to the IR stimulation. Here $\lambda_{IR} = \sigma_{IR}I$ is the infrared optical stimulation probability (s^{-1}) which is proportional to the intensity I of the IR light (photons per cm^2 per s), and to the IR stimulation cross section σ_{IR} (cm^2). The term $n_e(t)s$ in equations (1) and (2) describes the rate of change of the concentration of excited electrons $n_e(t)$, due to the possibility of electronic transitions from the excited state back into the ground state. The mathematical form of this term is determined from the principle of detailed balance (see for example, Chen and McKeever, 1997; Chen and Pagonis, 2011).

Equation (3) expresses the observed luminescence intensity as the product of the concentration of electrons $n_e(t)$ in the excited state, and the probability of recombination Γ (in s^{-1}). The time-dependent concentration of holes is denoted by $m(t)$, and is related to the electron concentrations at all times by the conservation of charge:

$$m(t) = n_t(t) + n_e(t) \quad (4)$$

In published localized models for thermoluminescence (TL), the probability of recombination Γ is usually considered to be a constant quantity, since the electron in the excited state is assumed to be able to interact only with the next neighboring holes/recombination centers. In the case of feldspars this recombination probability Γ varies according to the tunneling process (see the extensive discussion in Thomsen et al., 2008).

From the quantum mechanical theory of tunneling, it is known that the mean lifetime τ of the tunneling process is related to a frequency factor s' and to the tunneling distance r by the equation (Huntley, 2006):

$$\tau = \frac{1}{s'}e^{\alpha r} \quad (5)$$

where α is a constant with the dimensions of inverse distance. The probability of recombination Γ (in s^{-1}) is given by the inverse of the luminescence lifetime:

$$\Gamma = s'e^{-\alpha r} \quad (6)$$

From a physical point of view, we may expect that the tunneling distance r between the electron and hole will depend on the concentration of holes $m(t)$ in the material. This suggests the possibility of using a time-dependent empirical function $\Gamma(t)$ of the form:

$$\Gamma(t) = \gamma e^{-f(m)}, \quad (7)$$

where γ is an empirical constant to be determined by fitting the experimental data, and the time-dependent function $f(m)$ represents some algebraic function of the concentration of holes $m(t)$ at any instant t .

We further require that this recombination probability $\Gamma(t)$ vary according to the following physical properties: at very long times t the concentration of holes $m(t)$ should approach zero, and therefore the corresponding recombination probability $\Gamma(t)$ should also approach zero. Also at time $t = 0$ the concentrations of available holes and electrons $n_t(0) = m(0)$ must be at a maximum, hence the recombination probability $\Gamma(t)$ should also be at its maximum value. These conditions lead us to use the following simple empirical mathematical form for the recombination probability:

$$\Gamma(t) = \gamma e^{-a \left[\left(\frac{m(0)}{m(t)} \right)^{1/3} - 1 \right]} \quad (8)$$

where a is a dimensionless positive proportionality factor which characterizes an unknown physical property of the electron–hole pair.

Equation (8) has the desired mathematical form similar to equation (6), and also has the required physical properties at large and small times:

$$\Gamma(0) = \gamma = \text{maximum}, \quad \text{and} \quad \Gamma(\infty) = 0. \quad (9)$$

The constants γ and a in equation (8) are treated as adjustable parameters in the model, in order to obtain the best possible fit to the experimental data.

It is emphasized that as in all empirically derived models, it is not possible to “prove” that equation (8) is the “correct” mathematical form of the recombination probability. We introduce this specific expression on an empirical basis, and its usefulness is shown by comparing it with the experimental data.

Perhaps the most detailed study of the applicability of the power-law type decay in luminescence signals from feldspars has been carried out by Baril (2002). Huntley (2006) developed a model for tunneling processes in solids, and showed that the luminescence intensity $I(t)$ observed during the tunneling process follows a power-law type expression of the form:

$$I(t) = ct^{-k} \quad (10)$$

where c is a constant, and the power-law exponent k has a value around 1.0. By taking the logarithms of both sides in equation (10) we obtain:

$$\ln I = \ln c - k \ln t. \quad (11)$$

In this paper we show that the results from the simulations are consistent with the experimentally reported power-law decay of luminescence from feldspars at longer times. Furthermore, we investigate how the power-law exponent k in equation (11) depends on the kinetic parameters of the model.

3. Results from the model

We simulate the IR stimulation of the feldspar sample by solving the system of differential equations (1)–(4), for the time interval $t = 0$ to $t = 5000$ s. The numerical values chosen for the parameters in the model are: $\lambda_{IR} = 0.06 \text{ s}^{-1}$, $s = 10^5 \text{ s}^{-1}$, $\gamma = 10^5 \text{ s}^{-1}$, $a = 35$ and the initial conditions are $n_t(0) = m(0) = 6 \times 10^{12} \text{ cm}^{-3}$, $n_e(0) = 0 \text{ cm}^{-3}$. The numerical values of the various parameters and their effect on the results of the simulation are discussed in the next section of this paper.

Fig. 2a shows the simulated IRSL signal with the above parameters, on a semilog scale. The inset of Fig. 2a shows the same simulated data on a linear-log scale. The simulated data in Fig. 2a shows clearly the existence of two distinct time intervals. The first interval corresponds to short IR stimulation times (at an

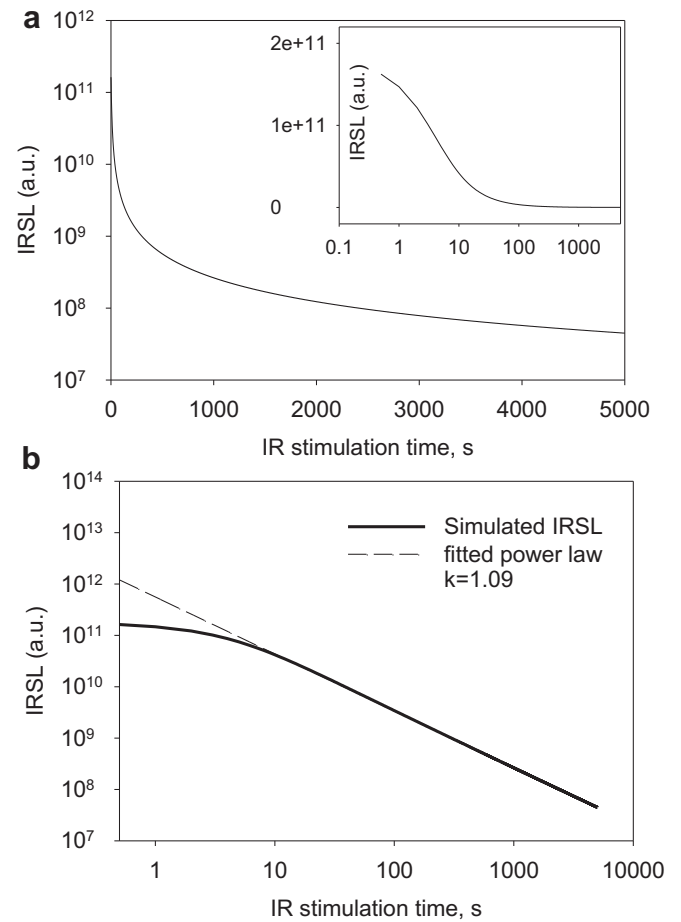


Fig. 2. (a) The simulated IRSL signal as a function of time on a semilog scale. The inset shows the same simulated data on a linear-log scale. The two distinct time regions can be clearly seen. (b) The same simulated data as in (a), on a log–log scale. The dashed line indicates a power-law fit to the data according to equation (11).

approximate value of $t < 10$ s), and is characterized by a very fast initial decay of the signal with time. The second interval for $t > 10$ s shows a much slower decay of the luminescence intensity with time. The existence of these two distinct time intervals in the simulation is in agreement with experimental results of Thomsen et al. (2011).

Fig. 2b shows the simulated data from Fig. 2a on a log–log scale. For large stimulation times, the $\ln I$ vs $\ln t$ graph is linear, indicating that the decay of the IRSL signal at large times follows a power-law type of decay, as described above in equations (10) and (11). The dashed line in Fig. 2b shows the best fit of the simulated data at large times with a power-law exponent $k = 1.09$.

We can obtain some physical insight into the nature of these two distinct time intervals in the IRSL signal, by examining the variation of the concentrations of electrons as a function of time. In Fig. 3a we show the concentration of trapped electrons $n_t(t)$ in the ground state and the corresponding concentration $n_e(t)$ of electrons in the excited state, as a function of time during the IR-stimulation process. The concentration $n_e(t)$ has been multiplied by a factor of 10^6 for easier visualization of the data. The concentration $n_t(t)$ in the ground state decreases continuously with time, due to the recombinations taking place between e–h pairs. The corresponding concentration $n_e(t)$ in the excited state increases initially, reaches a maximum at ~ 10 s, and subsequently decreases continuously with time at approximately the same time rate as $n_t(t)$.

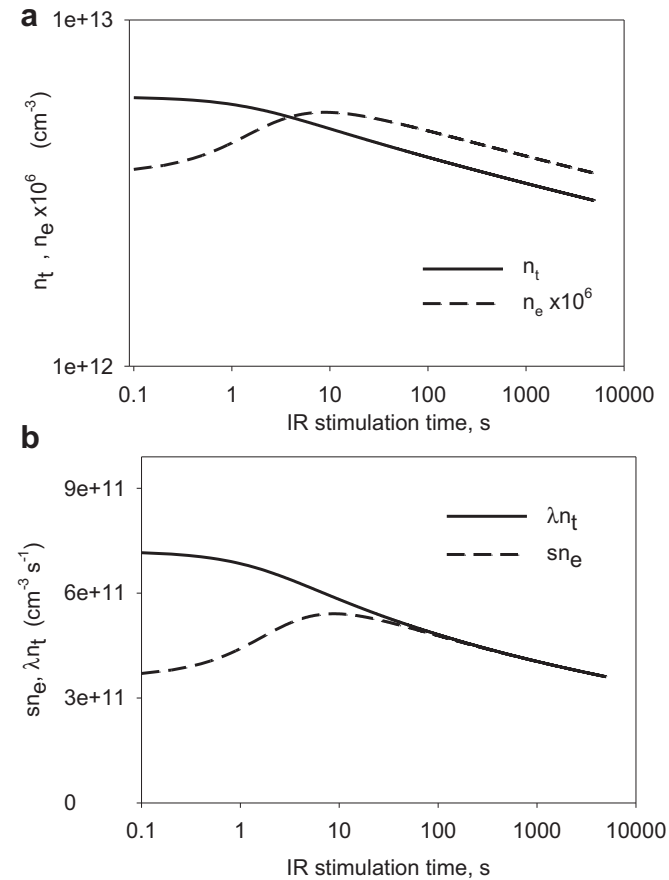


Fig. 3. (a) The concentrations of electrons in the ground state $n_t(t)$, and in the excited state $n_e(t)$ as a function of time during the IR stimulation. The latter is multiplied by a factor of 10^6 for visualization purposes. (b) The two terms appearing in equation (1) are plotted as a function of time.

Fig. 3b shows a similar behavior for the two terms $\lambda_{IR} n_t(t)$ and $n_e(t)s$ appearing in equation (1), as a function of time. For small times ($t < 10$ s), the infrared stimulation term $\lambda_{IR} n_t(t)$ decreases with time, while the excited-to-ground state transition term $n_e(t)s$ increases within the same time interval. At $t \sim 100$ s the two terms become practically equal and for $t > 100$ s they remain practically equal to each other, while they both decrease at the same rate. After the initial interval in which rapid change takes place, the two terms $-\lambda_{IR} n_t(t)$ and $n_e(t)s$ in equation (1) reach equilibrium. For long times these two terms remain in equilibrium, while they both decrease at a much slower rate.

We conclude that the simulated data of Fig. 3 explain the existence of two distinct time intervals in the IRSL signal. The initial fast decay corresponds to the two terms in equation (1) gradually reaching equilibrium. After equilibrium is reached between the two terms, the decay of the simulated IRSL signal is characterized by a much slower recombination rate, which can be described by a power-law type of equation.

Further insight into the processes taking place during the tunneling transitions is obtained from Fig. 4a, which shows the time variation of the percent ratio $n_t(t)/n_t(0)$ of the remaining electron–hole pairs (e–h) during the simulated IRSL process. Several simulated curves $n_t(t)/n_t(0)$ are shown in Fig. 4a; these were obtained by changing the probability of IR stimulation λ_{IR} in equation (1), by a few orders of magnitude. Fig. 4b shows similarly several of the corresponding IRSL signals obtained by varying λ_{IR} .

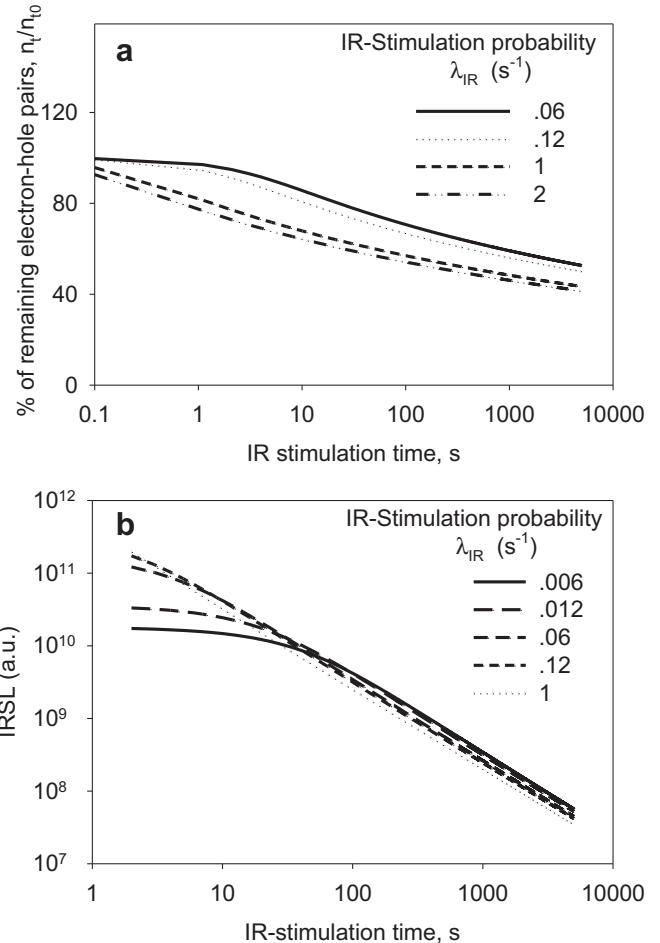


Fig. 4. (a) Simulated results showing the percent of remaining electron–hole pairs during the IR stimulation process, for different IR-stimulation probabilities. Experimentally this type of measurement is carried out by varying the power of the IR stimulating source. (b) Simulated IRSL curves for different IR-stimulation probabilities. The overall shape of the curves does not change significantly at longer stimulation times.

By inspection of the dotted curve obtained with $\lambda_{IR} = 0.12 \text{ s}^{-1}$ in Fig. 4a, we can obtain a physical insight into how the rate of the recombination processes changes along the IRSL curves. During the initial time interval, the percent ratio of remaining electron–hole pairs decreases rapidly, from 100% at time $t = 0$ decreasing to 65% of electron–hole pairs remaining at longer times $t = 200$ s. Clearly in this initial time interval only 35% of the initial concentration of e–h pairs have tunneled through the energy barrier, and have recombined radiatively. For large IR stimulation times the tunneling process takes place at a very reduced rate, so that the percent ratio of remaining e–h pairs decreases to $\sim 50\%$ within this large time interval. Therefore only an additional 15% of e–h pairs has tunneled within the time interval $t = 200$ s to $t = 5000$ s. Most notably, Fig. 4a shows that even after a time interval of 5000 s there are still $\sim 40\%$ of e–h pairs remaining in the system. This very slow recombination process occurring at long times explains why it is so difficult to completely erase the IRSL signal from feldspars; initially a large percentage of trapped electrons and holes recombines rapidly, but at longer times the tunneling process becomes very slow. In the next section we will show that within the simple model presented here, the slowly decaying part of the IRSL signal always follows a power-law type of decay.

Experimentally the type of measurement shown in Fig. 4b is carried out by varying the power of the IR stimulating source.

Fig. 5a shows experimental data obtained by Thomsen et al. (2011), using different IR-stimulation powers in their LED system. A coarse-grain sedimentary K-feldspar sample was measured (lab code: 981014). An aliquot of sample 981014 was given a dose of 7 Gy, preheated at 280 °C for 60 s and stimulated with IR at 50 °C for 10,000 s using LED power settings ranging between 1 and 100% ($\sim 1.35 \sim 135 \text{ mW/cm}^2$).

The experimental data are compared with the simulated data from the model, and very good agreement is found between the model and experiment. The simulated solid curves in Fig. 5a have been multiplied by an appropriate scaling factor, for comparison purposes. By increasing the power of the IR-LEDs, very significant changes occur mostly in the initial part of the IRSL signal, in which the rapid recombination rate prevails. The slower part of the IRSL signal at longer times is affected much less by changes in the IR power, in both the simulated and experimental data. The model parameters used to obtain the simulated data in Fig. 5a are: $s = 10^5 \text{ s}^{-1}$, $\gamma = 5 \times 10^5 \text{ s}^{-1}$, $a = 35$ and the initial conditions are $n_t(0) = m(0) = 6 \times 10^{12} \text{ cm}^{-3}$, $n_e(0) = 0 \text{ cm}^{-3}$.

Another detailed example of comparing experimental and simulated data is shown in Fig. 5b, for a different feldspar sample. The luminescence signals of this K-rich sediment extract (laboratory code 951020), were recently studied in Jain and Ankjærgaard (2011). The sample was given a dose of 45 Gy and subsequently

preheated to 250 °C for 60 s, prior to measurement of the IRSL signal at 50 °C. An excellent fit shown as a solid line through the experimental data is obtained using the model, for the complete time interval $t = 0$ to $t = 5000$ s. The simulated and experimental data in Fig. 5b are normalized to the first point in the experimental data. A small but finite constant signal has been added to the simulated data; this small signal could represent the experimental “background”, but also could represent a significant contribution from the band-tail states.

The model parameters used to obtain the simulated data in Fig. 5b are: $\lambda_{IR} = 0.06 \text{ s}^{-1}$, $s = 10^5 \text{ s}^{-1}$, $\gamma = 10^5 \text{ s}^{-1}$, $a = 35$, and the initial conditions are $n_t(0) = m(0) = 6 \times 10^{12} \text{ cm}^{-3}$, $n_e(0) = 0 \text{ cm}^{-3}$.

In the next section we study the effect of the various parameters on the results from the model. Our goal is (a) to determine which parameters have the most effect on the shape of the simulated IRSL signals, and (b) to further investigate the power-law of decay of the IRSL signal.

4. Effects of the various parameters on the simulated IRSL signals

We start by examining the numerical values of the frequency parameters λ_{IR} , s which appear in the system of equations (1)–(3). What is important in describing the behavior of the system of equations is not so much the absolute values of these parameters, but rather their numerical dimensionless ratio γ/s . These ratios represent the ratios of possible transition probabilities for electrons in the ground state and the excited state, correspondingly.

The value of the IR-stimulation parameter $\lambda_{IR} = 0.12 \text{ s}^{-1}$ was chosen in the simulation so that the simulated IRSL curve in Fig. 2a decays at similar rates as in typical experimental IRSL curves. The value of the frequency factors $s = \gamma = 10^5 \text{ s}^{-1}$ was chosen arbitrarily in the model, but is typical of frequency factors for localized processes. The value of the dimensionless parameter $a = 35$ in equation (8) was chosen so that the simulated data fits best the typical experimental data.

In Fig. 6a we show the effect of changing the ratio γ/s on the results of the model, by varying this ratio from $\gamma/s = 10^{-3}$ up to value of 10^2 . The simulation results show that this ratio affects mostly the initial part of the IRSL curve; for large stimulation times t , all simulated IRSL curves in Fig. 6a exhibit the power-law of luminescence decay. The values of the power exponent k obtained by fitting the simulated data of Fig. 6a are practically constant, with a very small random variation between $k = 1.03$ and 1.08 . We conclude that within this model, the power-law exponent k depends very weakly on the ratio γ/s , even though this ratio is varied over 5 orders of magnitude in the simulations. It is noted that the quantity γ/s does not depend on the experimental conditions, but rather is a physical property of the e–h pair.

In Fig. 6b we show the effect of changing the dimensionless parameter a on the results of the simulation. This parameter describes the unknown physical properties of the e–h pair relating to the tunneling process. The values of the power exponent k obtained by fitting the simulated data of Fig. 6b show a very small systematic decrease with the value of a , from $k = 1.09$ and $k = 0.96$. We conclude that within this model, the power-law exponent k depends rather weakly on the kinetic parameter a .

Finally we consider the effect of changing the initial concentration $n_t(0) = m(0)$ of e–h pairs on the results of the model, by varying this parameter within several orders of magnitude. The simulations show that changing the initial concentrations affects the magnitude of the IRSL signal, while the shape of the IRSL curve remains the same.

In conclusion, the simulated data in this paper show clearly that in all cases simulated here, and for a wide range of numerical values

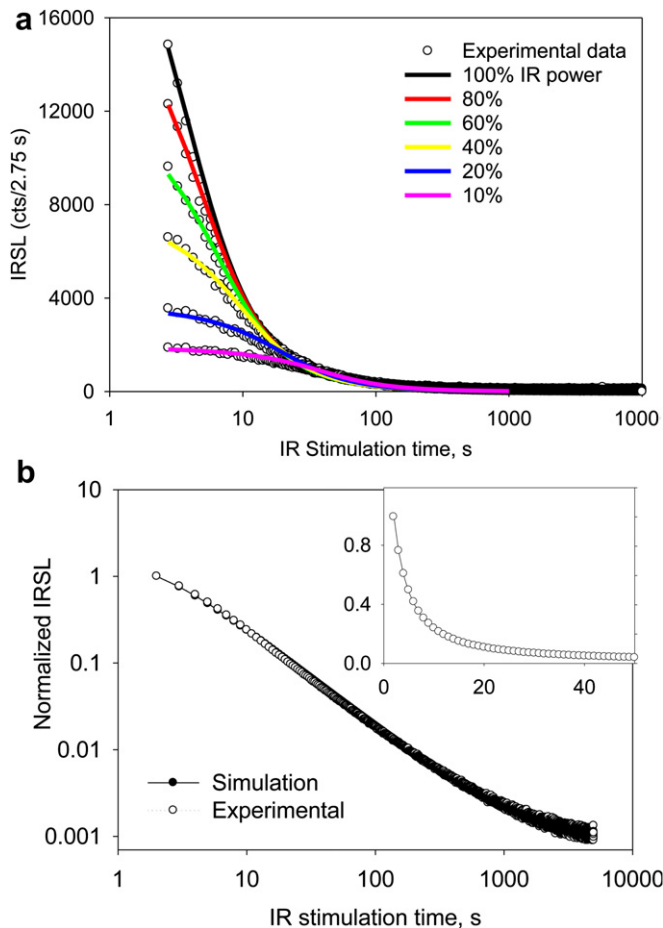


Fig. 5. (a) The experimental data of Thomsen et al. (2011), obtained using different powers of their IR LEDs. The simulated data are shown as solid lines. (b) A different set of experimental data for a K-rich feldspar sample. The experimental IR power is set at 100%. The inset shows the same experimental data for short IR stimulation times, on a linear scale. The offset is equal to the average of the last 100 channels in the IRSL signal.

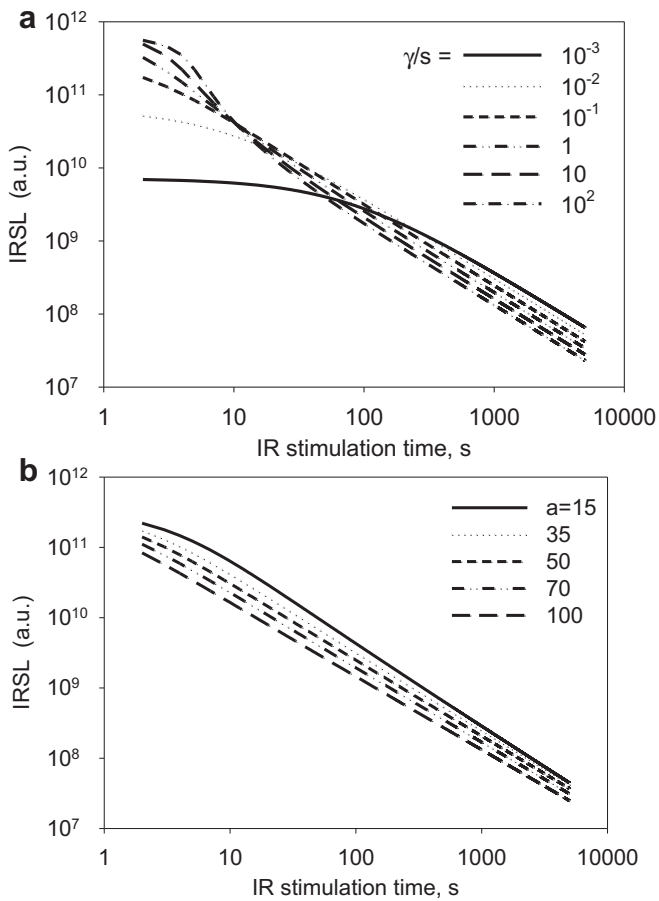


Fig. 6. (a) Simulated IRSL curves for different values of the ratio γ/s , from 10^{-3} to 10^2 . (b) Simulated IRSL curves for different values of an unknown physical property of e–h pair a in equation (9), on a log–log scale showing the linear regions of the power-law decay. The power-law exponent k obtained by fitting the power-law equation (10) to the simulated data in (a) and (b) depends only very weakly on the value of the parameters γ/s and a in the model.

of the parameters in the model, the shape of the IRSL curves does not change drastically. Of all the parameters varied in the model, the dimensionless parameter a has the largest effect on the shape of the IRSL curves.

5. Discussion and conclusions

The exact mathematical shape of the CW–IRSL curves is an open research question. Specifically, it is unclear whether the luminescence signals at long excitation times are better fitted with the power-law, or with a stretched exponential function, or even with some other “long-tailed” mathematical function. However, it is interesting to note that there has been some previous work on this subject: the PhD work by Baril (2002) contains a rather extensive discussion and study of the power-law, as applied to several types of luminescence signals from feldspars. In this paper we examined the possibility of obtaining the luminescence decay law based on the system of differential equations describing electronic trafficking between the excited state, the ground state and the luminescence center.

The model explains the experimental fact that the initial part of IRSL decay curves does not follow the power-law of luminescence decay. Two limitations of the current model are: (a) the absence of a role in the model for the band-tail states which are known to be present in feldspars, and (b) the absence of a mathematical

description of the effect of stimulating temperature on the shape of CW–IRSL curves. For example, Poolton et al. (2009) and Jain and Ankjærgaard (2011) demonstrated in their experimental work that band-tail states play a substantial role in the IRSL mechanism. At low temperatures ~ 10 K it is believed that the band-tail states are “frozen” and tunneling constitutes the main IRSL mechanism (Poolton et al., 2009). It has also been suggested that at higher temperatures the contribution of the band-tail states to the IRSL signal becomes more important.

In the model presented in this paper, the initial fast decay of the IRSL signal is explained on the basis of equilibrium being reached gradually between the two mathematical terms in equation (1). In the work of Thomsen et al. (2008), this initial fast decay was interpreted as due to recombinations taking place between nearby e–h pairs, while the slower part of the IRSL signal was due to recombinations between pairs located farther apart. It is unclear whether these two explanations of the shape of the IRSL curves are equivalent from a physical point of view, and further experimental and modeling work is necessary to clarify these points.

In this paper only experimental data obtained from K-feldspar are used for comparison, and other types of feldspar IRSL signals have not been tested. Clearly more extensive experimental and simulation work is needed to ascertain whether the simple model in this paper also describes the IRSL decay curves from other feldspar samples.

Acknowledgements

We thank Dr. Kristina Thomsen for providing us with a digital copy of the experimental data shown in Fig. 5. Dr. Vasilis Pagonis is also grateful for the financial support of the National Laboratory for Sustainable Energy, in Roskilde, Denmark during his visit in October 2010.

References

- Ankjærgaard, C., Jain, M., Kalchgruber, R., Lapp, T., Klein, D., McKeever, S.W.S., Murray, A.S., Morthekai, P., 2009. Further investigations into pulsed optically stimulated luminescence from feldspars using blue and green light. *Radiat. Meas.* 44, 576–581.
- Bailiff, I.K., Poolton, N.R.J., 1991. Studies of charge transfer mechanisms in feldspars. *Nucl. Tracks Radiat. Meas.* 18, 111–118.
- Baril, M.R., 2002. Spectral investigations of luminescence in feldspars. Ph.D. Thesis, Simon Fraser University, Burnaby, BC, Canada. Available online at: www.cfh.hawaii.edu/~baril/Temp/baril_phdthesis.pdf.
- Baril, M.R., Huntley, D.J., 2003. Optical excitation spectra of trapped electrons in irradiated feldspars. *J. Phys. Cond. Matt.* 15, 8011–8027.
- Bøtter-Jensen, L., McKeever, S.W.S., Wintle, A.G., 2003. *Optically Stimulated Luminescence Dosimetry*. Elsevier, Amsterdam.
- Chen, R., McKeever, S.W.S., 1997. *Theory of Thermoluminescence and Related Phenomena*. World Scientific Publications, London, NJ, Singapore.
- Chen, R., Pagonis, V., 2011. *Thermally and Optically Stimulated Luminescence: a Simulation Approach*. Wiley and Sons, Chichester.
- Delbecq, C.J., Toyozawa, Y., Yuster, P.H., 1974. Tunneling recombination of trapped electrons and holes in KCl: AgCl and KCl: TiCl. *Phys. Rev.* B9, 4497–4505.
- Duller, G.A.T., Bøtter-Jensen, L., 1993. Luminescence from potassium feldspar stimulated by infrared and green light. *Radiat. Prot. Dosim.* 47, 683–688.
- Huntley, D.J., 2006. An explanation of the power-law decay of luminescence. *J. Phys. Cond. Matt.* 18, 1359–1365.
- Huntley, D.J., Lamothe, M., 2001. Ubiquity of anomalous fading in K-feldspars and the measurement and correction for it in optical dating. *Canad. J. Earth Sci.* 38, 1093–1106.
- Jain, M., Ankjærgaard, C., 2011. Towards a non-fading signal in feldspar: insight into charge transport and tunneling from time-resolved optically stimulated luminescence. *Radiat. Meas.* 46, 292–309.
- Kars, R.H., Wallinga, J., Cohen, K.M., 2008. A new approach towards anomalous fading correction for feldspar IRSL dating-tests on samples in field saturation. *Radiat. Meas.* 43, 786–790.
- Larsen, A., Greilich, S., Jain, M., Murray, A.S., 2009. Developing a numerical simulation for fading in feldspar. *Radiat. Meas.* 44, 467–471.
- Li, B., Li, S.-H., 2010. Thermal stability of infrared stimulated luminescence of sedimentary K-feldspar. *Radiat. Meas.* 46, 29–36.

- Li, B., Li, S.-H., 2008. Investigations of the dose-dependent anomalous fading rate of feldspar from sediments. *J. Phys. D: Appl. Phys.* 41 (225502), 15. doi:10.1088/0022-3727/41/22/225502.
- Murray, A.S., Buylaert, J.P., Thomsen, K.J., Jain, M., 2009. The effect of preheating on the IRSL signal from feldspar. *Radiat. Meas.* 44, 554–559.
- Poolton, N.R.J., Bøtter-Jensen, L., Ypma, P.J.M., Johnsen, O., 1994. Influence of crystal structure on the optically stimulated luminescence properties of feldspars. *Radiat. Meas.* 23, 551–554.
- Poolton, N.R.J., Bøtter-Jensen, L., Johnsen, O., 1995. Thermo-optical properties of optically stimulated luminescence in feldspars. *Radiat. Meas.* 24, 531–534.
- Poolton, N.R.J., Kars, R.H., Wallinga, J., Bos, A.A.J., 2009. Direct evidence for the participation of band-tails and excited-state tunneling in the luminescence of irradiated feldspars. *J. Phys. Cond. Matt* 21, 485505.
- Poolton, N.R.J., Wallinga, J., Murray, A.S., Bulur, E., Bøtter-Jensen, L., 2002a. Electrons in feldspar I: on the wave function of electrons trapped at simple lattice defects. *Phys. Chem. Minerals* 29, 210–216.
- Poolton, N.R.J., Ozanyan, K.B., Wallinga, J., Murray, A.S., Bøtter-Jensen, L., 2002b. Electrons in feldspar II: a consideration of the influence of conduction band-tail states on luminescence processes. *Phys. Chem. Minerals* 29, 217–225.
- Templer, R.H., 1986. The localized transition model of anomalous fading. *Radiat. Prot. Dosim.* 17, 493–497.
- Thomsen, K.J., Murray, A.S., Jain, M., Bøtter-Jensen, L., 2008. Laboratory fading rates of various luminescence signals from feldspar-rich sediment extracts. *Radiat. Meas.* 43, 1474–1486.
- Thomsen, K.J., Murray, A.S., Jain, M., 2011. Stability of IRSL signals from sedimentary K-feldspar samples. *Geochronometria* 38, 1–13.
- Visocekas, R., 1985. Tunneling radiative recombination in labradorite: its association with anomalous fading of thermoluminescence. *Nucl. Tracks Radiat. Meas.* 10, 521–529.
- Wintle, A.G., 1973. Anomalous fading of thermoluminescence in mineral samples. *Nature* 245, 143–144.